

Mesoscopic BCS pairing in the repulsive 1d-Hubbard model

Luigi Amico and Andrea Mastellone

MATIS, INFM CNR and

Dipartimento di Metodologie Fisiche e Chimiche (DMFCI),

*Università di Catania, viale A. Doria 6, I-95125 Catania, Italy**

Andreas Osterloh

Institut für Theoretische Physik, Universität Hannover, 30167 Hannover, Germany†

(Dated: October 26, 2018)

Abstract

We study mesoscopic pairing in the one dimensional repulsive Hubbard model and its interplay with the BCS model in the canonical ensemble. The key tool is comparing the Bethe ansatz equations of the two models in the limit of small Coulomb repulsion. For the ordinary Hubbard interaction the BCS Bethe equations with infinite pairing coupling are recovered; a finite pairing is obtained by considering a further density-dependent phase-correlation in the hopping amplitude of the Hubbard model. We find that spin degrees of freedom in the Hubbard ground state are arranged in a state of the BCS type, where the Cooper-pairs form an non-condensed liquid on a “lattice” of single particle energies provided by the Hubbard charge degrees of freedom; the condensation in the BCS ground state corresponds to Hubbard excitations constituted by a sea of spin singlets.

PACS numbers: 74.78.Na,04.20.Jb

I. INTRODUCTION

Intensive analysis has been devoted to trace pairing phenomena in strongly interacting electronic models^{1,2,3}. Most of the motivations come from studies in high- T_c superconductivity for which it is highly desirable that pairing mechanisms are automatically encoded in the interaction. The Hubbard model constitutes the prototype of the class of models of interest in the subject⁴. It describes a lattice gas of itinerant electrons experiencing an on-site Coulomb interaction. So far, the evidence of pair-pair correlation is ambiguous both for repulsive and attractive Hubbard interaction^{5,6}. Here we focus on the Hubbard ($1d$) chains, with repulsive interaction⁷. Not only does a $1d$ analysis provide a unique theoretical lab to predict the behavior of compounds in higher dimension, but current technology actually admits quasi- $1d$ superconductors to be fabricated; finally, there is evidence that the stripe ordered domains gives effectively a $1d$ character to the phenomenology of even many superconducting $3d$ -compounds⁸. However, how the superconductivity does arise from stripes still constitutes an open problem. Assuming that the electronic properties of the stripe-domains can be captured by repulsive Hubbard-like models, effective pair-formation can be studied by means of the pair binding energy E_{pb} , detecting an energy gain whenever an electron-electron attraction is established into the system^{9,10,11}. In particular, E_{pb} was studied for the ground state (GS) of the *finite* $1d$ Hubbard model and it turned out that the repulsive local interaction can be over-screened, leaving an effective attraction among the electrons¹¹. This phenomenon was called mesoscopic pairing. An important motivation for us is to single out a *pairing of the BCS type* in the mesoscopic pairing of the Hubbard model. The attempt to trace BCS pairing within the Hubbard type models is not new, and it has been well studied in the physical community, mainly for attractive interaction. A common feature of such studies⁶ (with the exception of the variational study in Ref. 12) is that the analysis was done in the grand-canonical ensemble, involving mean field BCS (that is exact in thermodynamic limit¹³). The scenario changes in the canonical ensemble where the BCS gap vanishes identically, the “superconducting phase” is dominated by quantum fluctuations¹⁴ and the mean field BCS theory is inadequate¹⁵. On the other hand, the canonical analysis is a natural tool to study the mesoscopic BCS pairing in the Hubbard model. This choice in the context of the stripe physics is supported by various experimental evidences. Stripe ordered domains in superconducting nano-powders were detected in Ref.

16; fragmented nano-stripes ($10 - 20$ nanometers long) were clearly noticed also in bulk high-T superconductors¹⁷. We use the Bethe ansatz solution of the BCS model to compare the two pictures in the canonical ensemble. The exact solution of the BCS model was found by Richardson¹⁸ in 1963, but went unnoticed to the condensed matter community. It was discovered only recently to study the superconductivity at nanoscale^{14,15}.

The paper is organized in the following manner. In the next section we introduce the Hubbard model and its Bethe Ansatz due to Lieb and Wu. In section III a *formal* correspondence is established for $U \rightarrow 0^+$, where the spin degrees of freedom (the spin “quasi-momenta”) in the Hubbard GS can be seen as Cooper-pair quasi-energies corresponding to certain excitations of the BCS model. A finite pairing coupling can be achieved by considering certain gauge-field correlated-hopping in the Hubbard model, as shown in the section IV. The correspondence of the BCS GS to a “sea” of spin singlets on top of the Hubbard GS, is discussed in section V. The role of the BCS pairing in the mesoscopic pair-binding is discerned in the section VI. Finally, section VII is devoted to our conclusions, and the discussion of some physical implications.

II. THE HUBBARD MODEL

We consider a Hubbard chain of length L , with $N = N_\uparrow + N_\downarrow$ particles $M = N_\downarrow$ spin down, and periodic boundary conditions. Formulated in second quantization, the Hamiltonian is

$$H = -t \sum_{j=1}^L (c_{j+1,\sigma}^\dagger c_{j,\sigma} + h.c.) + U \sum_{j=1}^L n_{j,\uparrow} n_{j,\downarrow}, \quad (1)$$

where $\{c_{j,\sigma}, c_{l,\sigma'}^\dagger\} = \delta_{\sigma,\sigma'} \delta_{j,l}$, $\{c_{j,\sigma}, c_{l,\sigma'}\} = 0$, and $n_{l,\sigma} := c_{l,\sigma}^\dagger c_{l,\sigma}$; $\sigma = \{\uparrow, \downarrow\}$ is the electronic spin; U and t (we set $t = 1$) are the Coulomb interaction and the hopping amplitude respectively. The many-body wave function

$$|\psi\rangle = \frac{1}{\sqrt{N!}} \sum_{1 \leq j_1 \leq \dots \leq j_N \leq L} \sum_{\mathcal{S}_N} \psi(j_1, \dots, j_N | \pi) c_{j_1 \sigma_{\pi(1)}}^\dagger \dots c_{j_N \sigma_{\pi(N)}}^\dagger |0\rangle, \quad (2)$$

brings Eq. (1) to the first quantized spectral problem $\mathcal{H}\psi = \mathcal{E}\psi$, that can be solved by the Bethe ansatz¹⁹

$$\psi(j_1, \dots, j_N | \pi) = \sum_{Q \in \mathcal{S}_N} A_\pi(Q) \exp \left\{ i \sum_{l=1}^N k_{Q(l)} j_l \right\}, \quad (3)$$

$$A_\pi(Q) = \sum_{R \in \mathcal{S}_M} G(R) \prod_{\alpha=1}^M F(\lambda_{R(\alpha)}, y_\alpha | Q), \quad (4)$$

$$F(\lambda, y | Q) = \frac{2iU}{\lambda - \sin k_y + iU} \prod_{l=1}^{y-1} \frac{\lambda - \sin k_l - iU}{\lambda - \sin k_l + iU}, \quad (5)$$

$$G(R) = \prod_{1 \leq \alpha < \beta \leq M} \frac{\lambda_\alpha - \lambda_\beta - 2iU}{\lambda_\alpha - \lambda_\beta}. \quad (6)$$

In these equations π labels a permutation of the indices in the configuration space, whereas Q and R label permutations in the $\{k\}$, $\{\lambda\}$ values in the symmetric group \mathcal{S}_N and \mathcal{S}_M respectively.

The exact energy and momentum of the model^{7,19}

$$E = -2 \sum_{j=1}^N \cos k_j \quad P = \sum_{j=1}^N k_j \quad (7)$$

are given in terms of charge-momenta k_j , solutions of the Lieb-Wu Bethe Equations (BE)²⁰

$$e^{iLk_j} = \prod_{\alpha=1}^M \frac{\sin k_j - \lambda_\alpha + \frac{iU}{4}}{\sin k_j - \lambda_\alpha - \frac{iU}{4}} \quad (8)$$

$$\prod_{j=1}^N \frac{\sin k_j - \lambda_\alpha + \frac{iU}{4}}{\sin k_j - \lambda_\alpha - \frac{iU}{4}} = \prod_{\substack{\beta=1 \\ \beta \neq \alpha}}^M \frac{\lambda_\alpha - \lambda_\beta - \frac{iU}{2}}{\lambda_\alpha - \lambda_\beta + \frac{iU}{2}}, \quad (9)$$

where $j \in \{1, 2, \dots, N\}$ and $\alpha \in \{1, 2, \dots, M\}$.

The equations (7), (8), and (9) constitute the exact solution of the Hubbard model both for repulsive and attractive interactions. We focus on the limit $U \rightarrow 0^+$. The result of such operation on Eqs. (7), (8) and (9) depends on the actual configurations of the charge and spin rapidities k, λ . For numerics, systems up to $N = 100$ electrons have been considered.

III. HUBBARD GROUND STATE FOR VANISHING INTERACTION

Here we consider the half-filled chain, and $N = 2M$, N even. For $U > 0$ the GS is characterized by real k and λ , where any λ_α is trapped between two $\sin k_\alpha$. Systems

with $N = 4n$ electrons are characterized by degenerate $\sin k = 0$ (see the central cluster of Fig. 1 (a)). At small U the two $\sin k_\alpha$'s are arranged symmetrically around λ_α as $|\lambda_j - \sin k_j| \simeq C_j U^{1/2} + D_j U$ where C_j and D_j are numerical coefficients; from the numerical analysis we find $D_j = 1/4$. We further assume the quasi-momenta having the following behavior $k_j \simeq k_j^{(0)} + U^{1/2} k_j^{(1/2)} + U k_j^{(1)}$; this assumption will be confirmed by our numerical studies. The limit $U \rightarrow 0^+$ of Eqs. (8) and (9) reads^{19,21}

$$e^{ik_j^{(0)} L} = 1, \quad (10)$$

$$k_j^{(1)} L = \frac{1}{2} \sum_\alpha' \frac{1}{\sin k_j^{(0)} - \lambda_\alpha}, \quad (11)$$

$$\sum_{\beta \neq \alpha} \frac{2}{\lambda_\beta - \lambda_\alpha} - \sum_{j=1}^N \frac{1}{\sin k_j - \lambda_\alpha} = 0. \quad (12)$$

and $k_j^{(1/2)} L = 1/2C_j$. \sum' in Eq. (11) indicates that the term $\sin k_\alpha$ is omitted. Notice that U has to be small in order that both $|U^{1/2} k_j^{(1/2)} L| \ll 1$ and $|U k_j^{(1)} L| \ll 1$ are satisfied and that degenerate $\sin k_j$ may occur in Eq. (12) (see Fig. 1).

The Bethe ansatz wavefunction in the limit of vanishing U is¹⁹

$$\lim_{U \rightarrow 0} \frac{A_\pi(Q)}{(2iU)^M} = \sum_{R \in \mathcal{S}_M} \prod_{\alpha=1}^M \frac{1}{\lambda_{R(\alpha)} - \sin[k_{Q(y_\alpha)}]} \quad (13)$$

The relevance of this limit resides in the following observation. The Eqs. (12) are known as the Gaudin equations. They play an important role in the exact solution of the BCS model at infinite pairing coupling g . The BCS Hamiltonian for N_p time-reversed pairs in Ω single particle levels ε_j with pair degeneracy d_j reads²²

$$\begin{aligned} H_{BCS} &= \sum_m \sum_{j=1}^{\Omega} \varepsilon_j c_{j,m}^\dagger c_{j,m} - g \sum_{i,j=1}^{\Omega} \sum_{m,m'} c_{i,m}^\dagger c_{i,\bar{m}}^\dagger c_{j,\bar{m}'} c_{j,m'} \\ &= \sum_{j=1}^{\Omega} \varepsilon_j \tau_j, \quad \tau_j = \sum_{i \neq j} \frac{\vec{S}_i \cdot \vec{S}_j}{\varepsilon_i - \varepsilon_j} + \frac{1}{g} S_j^z, \end{aligned} \quad (14)$$

where $c_{j,m}^\dagger$ creates an electron in the state $|j; S_j, m\rangle$, $m \in \{1 \dots d_j\}$; $|j; S_j, \bar{m}\rangle$ is the time reversed state of $|j; S_j, m\rangle$. The operators $S_j^- := \sum_m c_{j,\bar{m}} c_{j,m}$, $S_j^+ := (S_j^-)^\dagger$, $S_j^z := (\sum_{m=-d_j}^{d_j} n_{jm} - d_j)/2$ form a $d_j/2$ dimensional representation of the $su(2)$ algebra. The second line of Eq. (14) establishes the relation between H_{BCS} and the twisted six-vertex models²³ through the Gaudin model²⁴, ultimately proving the integrability of the BCS model.

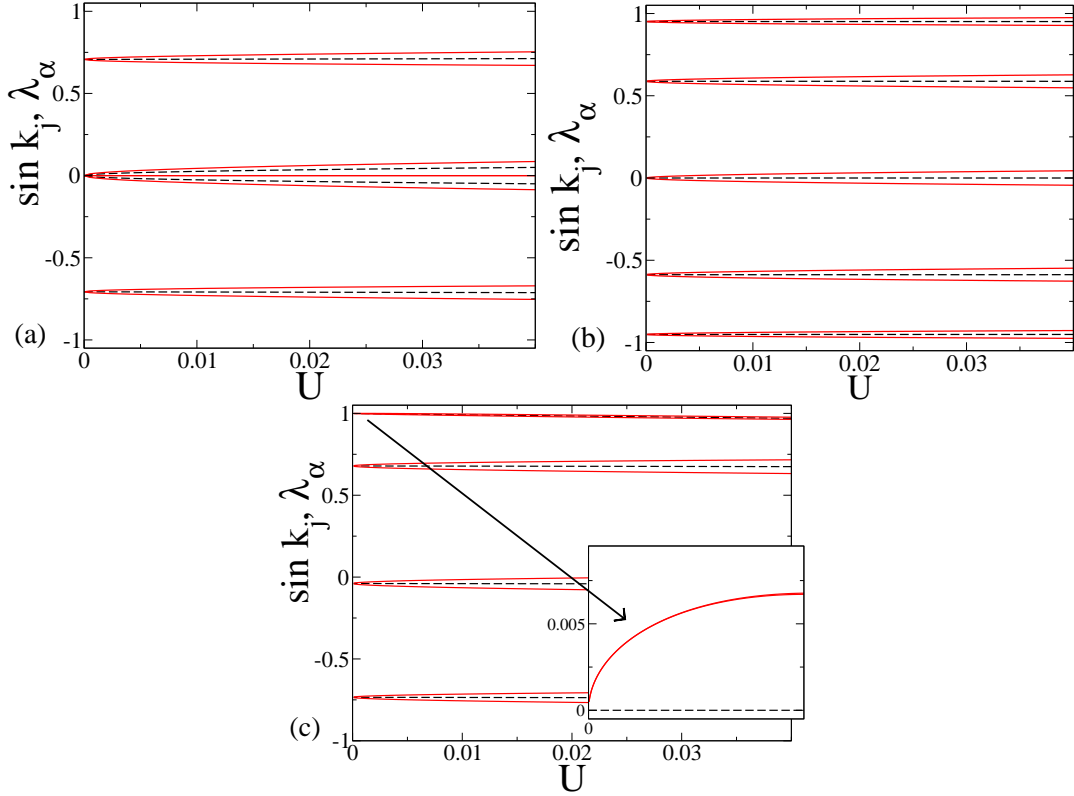


FIG. 1: The spin (λ_α , black dashed lines) and charge ($\sin k_j$, red solid lines) rapidities at $U/t \ll 1$, for a system with 8 (a) and 10 (b) electrons. A correlated hopping $\Phi_\sigma \neq 0$ removes the degeneration of the cluster at $k = 0$ for $N = 4n$ (c). In the upper cluster, though λ_α exhibits a slight dependence on U , the functional behavior of the difference $|\lambda_\alpha - \sin k_\alpha|$ remains the same (inset).

Its exact energy and eigenstates¹⁸ are

$$\mathcal{E}_{BCS} = \sum_{\alpha=1}^{N_p} e_\alpha + \sum_{i=1}^{N_b} \varepsilon_i \quad (15)$$

$$\frac{1}{g} - \sum_{j=1}^{\Omega} \frac{d_j}{2\varepsilon_j - e_\alpha} + \sum_{\beta \neq \alpha=1}^{N_p} \frac{2}{e_\beta - e_\alpha} = 0, \quad (16)$$

$$|\Psi\rangle = \sum_{R \in \mathcal{S}_{N_p}} \prod_{\alpha=1}^{N_p} \frac{1}{e_{R(\alpha)} - 2\varepsilon_{Q(y_\alpha)}} S_{R(\alpha)}^\dagger = \prod_{\alpha=1}^{N_p} \sum_{j=1}^{\Omega} \frac{S_j^\dagger}{e_\alpha - 2\varepsilon_j} |0\rangle \quad (17)$$

where the second sum in Eq.(15) runs over the set of N_b blocked levels, i.e. occupied by a single electron and not available to pair scattering. Different states in Eq. (17) correspond to different distributions of the e_α at $g = 0$ on the ε_j -configuration; in the BCS GS all ε_j 's are complex conjugates. The relation between Eqs. (16),(17) and Eqs. (12), (13) is evident identifying $2\varepsilon_j$ and e_α (the pairing quasi-energies) with $\sin k_j$ and λ_α respectively, Ω and N_p

playing the role of N and M . Eqs. (12) are obtained from Eq. (16) in the limit $g \rightarrow \infty$. Important for our purposes are the excitations of the BCS model characterized by real $\{e_\alpha\}$; it was noticed that in the canonical ensemble these can be obtained as the states in Eq. (17) corresponding to $\{e_\alpha\}$, *finite* solutions of the Gaudin equations²². Therefore we conclude that the spin-rapidities (all of them are real and finite) in the Hubbard GS are arranged along the configuration of the BCS excited state displayed in the Fig. 2.

IV. FINITE PAIRING

Now we show that a finite value of g can be obtained by adding a further interaction in the original Hubbard model, in form of correlated-hopping. The correlated hopping we consider corresponds to

$$t \rightarrow t \exp \left[i \sum_l (\alpha_{j,l}(\sigma) N_{l,-\sigma} + A_{j,l}(\sigma) N_{l,\sigma}) \right], \quad (18)$$

in Eq. (1). The Hubbard model with the correlated hopping Eq. (18) are of the Shastry-Schulz type²⁵. They were solved exactly for A, α obeying certain restrictions²⁶. It was demonstrated²⁶ that the effect of the correlated hopping is to twist the boundary conditions. The boundary phases are $\Phi_\sigma := \phi(\sigma) + \theta_{\uparrow\downarrow}(\sigma) N_{-\sigma} + \theta_{\uparrow\uparrow}(\sigma) (N_\sigma - 1)$, with $\phi(\sigma) = \sum_{j=1}^L A_{j,j}(\sigma)$, $\theta_{\uparrow\downarrow}(\sigma) = \sum_{j=1}^L \alpha_{j,m}(\sigma)$, $\theta_{\uparrow\uparrow}(\sigma) = \sum_{j \neq m-1,m}^L A_{j,m}(\sigma) + A_{m,m-1}(\sigma) + A_{m-1,m+1}(\sigma)$. The BE of the Schulz-Shastry models are obtained from the Lieb-Wu BE, by multiplying with the factors $e^{-i\Phi_\uparrow}$ and $e^{i(\Phi_\uparrow - \Phi_\downarrow)}$ the r.h.s. of the equations (8) and (9) respectively. To obtain a finite g , it is assumed also that $\Phi_\sigma \simeq \Phi_\sigma^{(0)} + U\Phi_\sigma^{(1)}$. For $-\pi \leq k_j < \pi$ we find that the conditions $\Phi_{\uparrow\downarrow}^{(0)} = \Phi_\uparrow^{(0)} - \Phi_\downarrow^{(0)} = 0$ and $|U\Phi_{\uparrow\downarrow}^{(1)}| \ll 1$ must be satisfied, in order to obtain the BE to zero order in U . The Eqs. (10) and (11) then modify into

$$\begin{aligned} e^{ik_j^{(0)} L} &= e^{-i\Phi_\uparrow^{(0)}}, \\ k_j^{(1)} L &= -\Phi_\uparrow^{(1)} + \frac{1}{2} \sum_\alpha' \frac{1}{\sin k_j^{(0)} - \lambda_\alpha}, \end{aligned}$$

and Eqs.(12) into

$$\frac{1}{g} - \sum_{j=1}^N \frac{1}{\sin k_j - \lambda_\alpha} + \sum_{\beta \neq \alpha=1}^M \frac{2}{\lambda_\beta - \lambda_\alpha} = 0, \quad (19)$$

with $g \equiv 1/(2\Phi_{\uparrow\downarrow}^{(1)})$. Thus the BE of the correlated hopping Hubbard model lead, in the limit $U \rightarrow 0^+$, to Richardson BE, Eq. (16). In the same limit the Eq. (7) is

$$E = \frac{2U\Phi_{\uparrow\downarrow}^{(1)}}{L} \sum_{\alpha=1}^M \lambda_{\alpha} + \text{const.}$$

with the constant being $UM(N - M + 1)/L - 2 \sum_{j=1}^N \cos k_j^{(0)} - (2U\Phi_{\uparrow}^{(1)}/L) \sum_{j=1}^N \sin k_j^{(0)}$. That is: for small U , the energy of the Hubbard model coincides (up to constants) with the energy of the BCS model, see Eq.(15).

The excitation of the BCS model corresponding to the Hubbard GS is achieved by filling the levels ε_j 's with a Cooper pair, leaving one empty level between two filled ones. In this way, the empty levels prevent the pairing parameters to form complex conjugate pairs. Such a BCS excitation is constituted by an non-condensed liquid of Cooper pairs (see the discussion in the next paragraph). The structure of these excitations is different for $N = 4n + 2$ and $N = 4n$. In the first case the ε_j are all non degenerate: $d_j = 1, \forall j$; for $N = 4n$, instead, the doubly degenerate Fermi energy correspond to a doubly degenerate ε_j , as one can see in the Figs. 1 and 2).

V. THE BCS GROUND STATE

The trait of the condensation of the Cooper pairs in the BCS GS is the emergence of complex conjugate e_{α} , solution of Eq. (16). In fact by resorting certain electrostatic analogy^{27,28} it can be proved that the thermodynamic limit of the Richardson's BE leads to the gap equation: $2G \int_{\Omega} \rho(\varepsilon) / \sqrt{(\varepsilon - a)(\varepsilon - b)} = 1$ where $\rho(\varepsilon)$ is the density of single particle levels; the parameters $a = \varepsilon_0 + i\Delta$ and $b = \varepsilon_0 - i\Delta$ are the the end points of the arc where the solutions of Eqs.(16) are disposed (see Fig.3; see also Refs. 22,29). Thus: the BCS gap (in the thermodynamic limit) is directly related to the maximum of the imaginary part of the e_{α} ^{22,28,29}. For large g all the e_{α} are complex conjugated pairs (with a single exception if N_p is odd); their real part is far below the lowest ε_j (see e.g. Ref. 22).

To find the Hubbard eigenstate corresponding to the BCS GS we insert into Eqs. (8), (9) the $e_{\alpha} (\equiv \lambda_{\alpha})$ configuration obtained by solving Eq. (19) with certain configuration of $\sin k_j^{(0)}$; this fixes the k_j , given the Φ_{σ} we have used for Eq. (19) with $|U\Phi_{\sigma}^{(1)}| \ll 1$. We found that all the k_j 's are real and non degenerate for non degenerate $\sin k_j^{(0)}$'s. (degenerate $\sin k_j^{(0)}$ correspond to degenerate k_j). Numerically we found that the mapping can be reliably

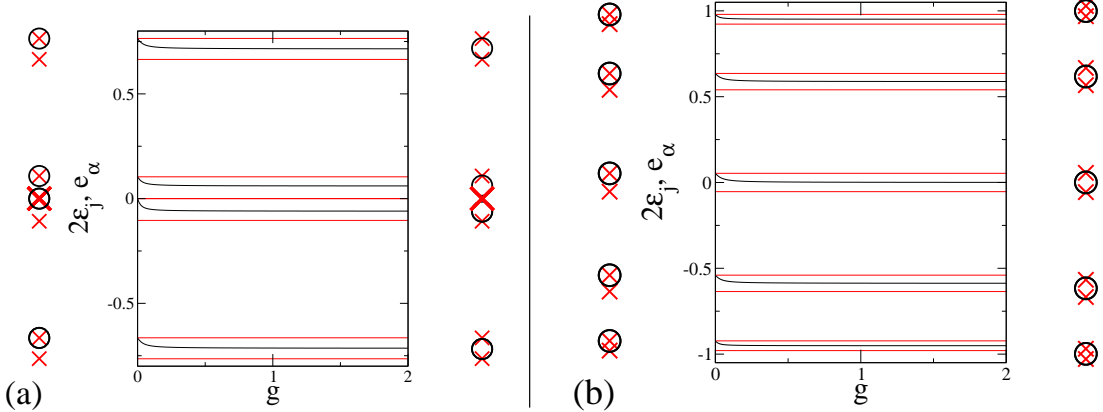


FIG. 2: BCS and Gaudin configurations leading to finite solutions at large pairing, for $N = 4n$ (a) and $N = 4n + 2$ (b) and $n = 2$. The plot shows the behavior of the pairing parameters while increasing g , black curves, whereas the single particle energies remain constant, red lines. On left sides of the plots, the initial configuration of the pairing parameters λ_α (black circles) on the energy levels $2\varepsilon_j$ (red crosses) is shown; on the right sides the final configuration is displayed. The latter are the charge and spin configurations corresponding to the ground state of the Hubbard model. The larger cross in plot (a) indicates the double degenerate level $2\varepsilon = 0$.

done for $U \lesssim 0.03$. It then turns out that $\sin k_j = \sin k_j^{(0)} + U\delta_j$; and $|\sin k - \lambda| \neq 0$ is always satisfied. These conditions imply that equation (19) characterizes also the excited Hubbard state under consideration. Summarizing, real k_j & complex conjugate λ_α pairs, solutions of the Richardson BE, satisfy the Lieb-Wu equations. We conclude that the BCS GS corresponds to a sea of spin singlets (Λ -2 strings) in the Hubbard chain. Such a state can be seen as a BCS condensation of spin rapidities. As an example of such result, the table shows the k, λ solution of both the BCS and the Hubbard GS BE for $U = 0.001$, $N = 6$, and $M = 3$.

$\sin k_j$	λ_α
-2.14679391, -1.09959633	-14.8060834
-0.052399128, 0.994798057	-11.722088 - i 11.1576888
2.04199559, 3.08919348	-11.722088 + i 11.1576888

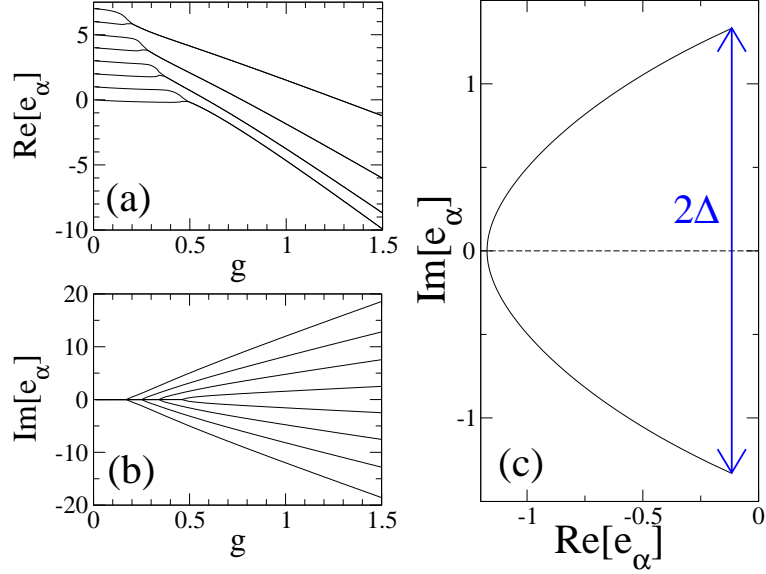


FIG. 3: (a) The real and (b) the imaginary part of the pairing parameters are shown as functions of the pairing strength g for a system with $N = 16$ electrons at half-filling in the BCS ground state configuration. In the thermodynamic limit the pairing parameters, being all complex conjugate at sufficiently large pairing, are arranged along arcs (see Ref. 29), where the distance between the end-points is the BCS gap 2Δ . Here we have set $g = 3.0$ and $N = 200$, with the single particle levels uniformly distributed in the range $[-1,1]$.

VI. MESOSCOPIC PAIRING

Here, we have a look at the pair binding energy $E_{pb} \doteq 2E(N+1) - E(N) - E(N+2)$. For the Hubbard GS, E_{pb} shows “super-even effects”^{9,11}. Effective pair attraction $E_{pb} > 0$ occurs for $N = 4n$ (n is integer), and it is related with a vanishing GS spin gap $\Delta_S \doteq E(N)_{S=1} - E(N)_{S=0}$ for $U \rightarrow 0^+$; for $N = 4n + 2$, $E_{pb} < 0$, corresponding to $\Delta_S > 0$ at small U . In Fig.(4) we present E_{pb} for the Hubbard and for Shastry-Schulz models. We observe that the correlated hopping, Eq. (18), washes out the super-even effects (see Fig.4); for $N = 4n + 2$ and $U > U_c$ $E_p > 0$ (see also Ref. 10); at small N we found that $U_c \propto N$. For larger N , U_c decreases (at $N = 50$, $U_c \approx 2.5$). The phenomenon will be analyzed elsewhere. The formation of Δ_S can be interpreted within the Hubbard-BCS correspondence: the state with $S = 1$ is obtained from $S = 0$ by breaking a BCS pair and thereby blocking single particle levels. In this scenario the super-even effect arises (see also Fig.5) because breaking a pair in the state with $N = 4n$ is energetically favorable,

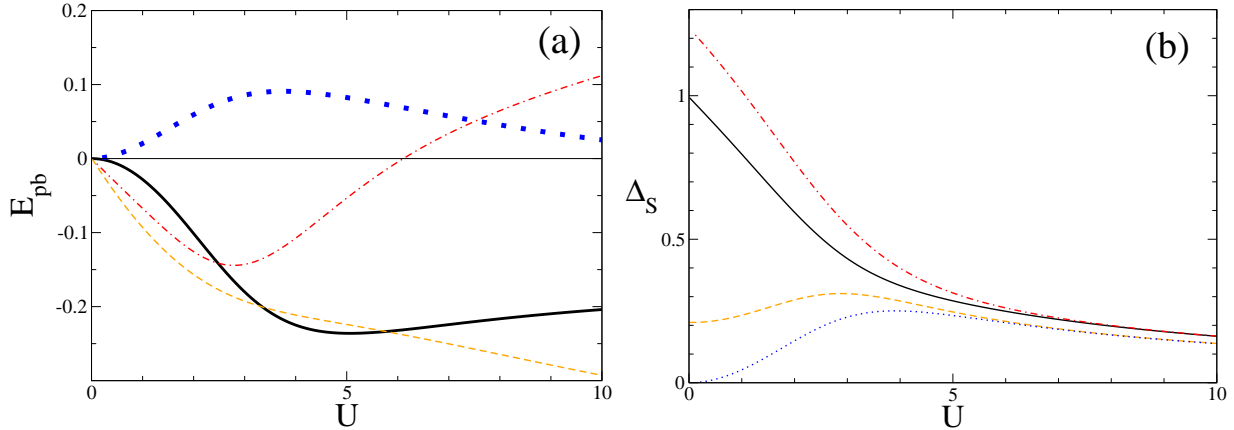


FIG. 4: The super-even effects for the pair binding energy E_{pb} (a) and the spin gap Δ_s (b). Thick and light lines are results for periodic and twisted boundaries respectively. $N = 10$: black solid line and red dotted-dashed line; $N = 12$: blue dotted line and orange dashed line. The boundary twist is set to $\Phi_{\uparrow}^{(0)} = \Phi_{\downarrow}^{(0)} = 0.2\pi$, $\Phi_{\uparrow}^{(1)} = 0.1\pi = 2\Phi_{\downarrow}^{(1)}$.

creating two blocked degenerate single particle levels, without kinetic energy extra cost. In contrast, for $N = 4n + 2$ the blocking of levels occurs at $k > k_F$. Away from half filling this is sufficient to cause an increase of the total energy; at half filling the levels are blocked in such a way that all the levels in the band are reshuffled, since breaking a pair at the Fermi energy causes the occupancy of the state at $k = 0$. We study the phenomenon by considering the pair correlation function $\Psi_j = |u_j|$, where $u_j \doteq \langle c_{j\bar{m}}^\dagger c_{j\bar{m}} c_{j\bar{m}} c_{j\bar{m}} \rangle$ detecting the fluctuational superconductivity in the canonical ensemble (in the thermodynamic limit Ψ_j becomes the BCS gap)¹⁴. Here we exploit the exact results achieved in Ref. 30 where $\Psi_j = |u_j|$ is calculated from a generating function³¹.

Exclusively for systems with pair attraction ($N = 4n$ with $\Phi_\sigma \equiv 0$) a dip at $k = 0$ is observed (Fig.6); this reflects the corresponding small energy gap required to occupy the $k = 0$ mode in the $S = 0 \rightarrow S = 1$ process.

VII. CONCLUSIONS

We proved that the exact solution of the BCS model can be obtained from the Bethe ansatz solution of the Hubbard model at vanishing U . At a formal level we comment that the amplitudes $A_\pi(Q)$ diagonalizing the 'spin sector' of the Hubbard model are, in

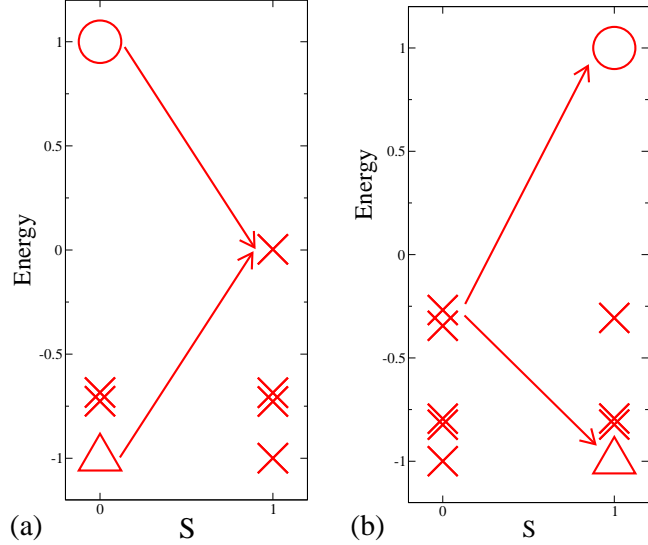


FIG. 5: The energy configuration ($-2 \cos k$) of the charge rapidities in the $S = 0, 1$ ground states for $N = 4n$ (a) and $N = 4n + 2$ (b) systems. The different symbols indicate the degeneracy of the levels: circle, cross and triangle stand for one, two and three-fold degenerate levels respectively. Note that the three-fold degenerate levels are more precisely “quasi-degenerate” ones: the energy difference cannot be resolved in the plot. At $N = 4n$, passing from $S = 0$ to $S = 1$ state two degenerate single particle levels are created and no additional energy is required (as shown by the arrows). Instead, at $N = 4n + 2$, at half filling the levels are reshuffled, a pair is broken at Fermi level and a $k = 0$ level is occupied (upper arrow).

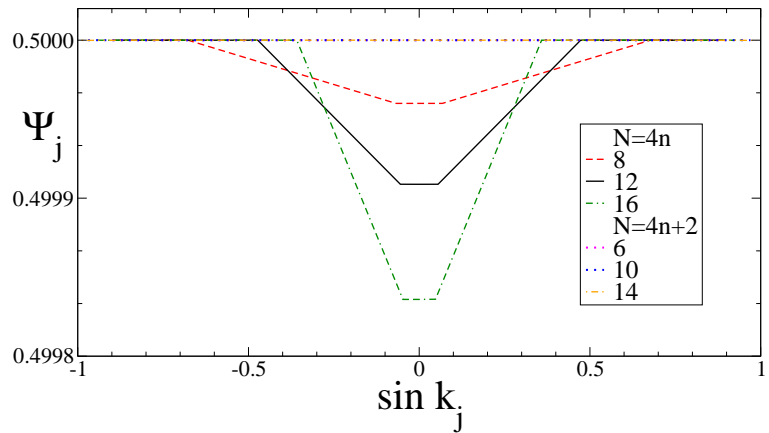


FIG. 6: The pairing correlator $\Psi_j = |u_j|$ is presented (in the thermodynamic limit Ψ_j would become the BCS gap). We notice the anomaly for $N = 4n$.

fact, eigenvectors of the transfer matrix of certain inhomogeneous six vertex models¹⁹. The relation between the Hubbard chain and the BCS model arises because the BCS model is itself a quasi-classical descendent of the inhomogeneous six vertex model²³. The Coulomb repulsion U/t plays the role of the quasi-classical parameter; the charge degrees of freedom $\{\sin k\}$ of the Hubbard model play the role of the inhomogeneities for the vertex models. In the BCS picture, they provide the “lattice” of single particle energies ε_j where the spin degrees of freedom, the spin “quasi-momenta” λ_α , can condense. The Hubbard ground state corresponds to a certain excited BCS state (see Fig.2). We noticed that also the Hubbard low lying spin excitations corresponds to states of the BCS type. In particular we have demonstrated that the BCS ground state of the spin rapidities reflects the formation of a sea of spin singlets in the Hubbard chain. In this scenario the super-even effective attraction in the Hubbard and in the Shastry-Schulz ground states can be understood in terms of pair-breaking excitations in the BCS model. We have demonstrated that BCS-correlators serve to study such parity effects.

The results obtained in this paper might be relevant for the analysis of the stripe order in the high- T_c compounds.

Acknowledgments

A. Di Lorenzo, F. Dolcini, G. Falci, R. Fazio, H. Frahm, A. Fubini, M. Roncaglia, and G. Sierra are acknowledged for discussions and support.

* Electronic address: lamico@dmfci.unict.it; URL: <http://fisica.ing.unict.it/~lamico>

† Electronic address: andreaso@itp.uni-hannover.de; URL: <http://www.itp.uni-hannover.de/~andreaso/>

¹ A.J. Leggett, *J. de Physique*, C7, **41**, 19 (1980); P. Nozières and S. Schmitt-Rink, *J. Low Temp. Phys.* **59**, 195 (1985).

² C.N. Yang, *Phys. Rev. Lett.* **63**, 2144 (1989).

³ M. Capone, *et al.*, *Science* **296**, 2364 (2002).

⁴ E.W. Carlson, *et al.*, “*The Physics of Conventional and Unconventional Superconductors.*” ed. by K. H. Bennemann and J. B. Ketterson (Springer-Verlag, Berlin, 2000)

⁵ A. Moreo, *Phys. Rev. B* **45**, 5059 (1992). 7464 (1997).

⁶ F. Marsiglio, Phys. Rev. B **55**, 575 (1997); W. Fettes, I. Morgenstern, and T. Husslein, Int. J. Mod. Phys. C **8**, 1037 (1997).

⁷ N. Andrei, “*Integrable models in condensed matter physics*”, in “Low dimensional quantum field theories for condensed matter physicist”, ed. S. Lundqvist, G. Morandi, and Yu Lu (World Scientific, Singapore, 1995).

⁸ X. J. Zhou *et al.*, Science **286**, 268 (1999).

⁹ V.J. Emery, S.A. Kivelson, and H.Q. Lin, Phys. Rev. Lett. **64**, 475 (1990).

¹⁰ R.M. Fye, M.J. Martins, and R.T. Scalettar, Phys. Rev. B **42**, 6809 (1990).

¹¹ S. Chakravarty and S. A. Kivelson, Phys. Rev. B **64**, 064511 (2001).

¹² K. Tanaka and F. Marsiglio, Phys. Rev. B **60**, 3508 (1999); see also N. Salwen, S.A. Sheets, and S.R. Cotanch, Phys. Rev. B **70**, 064511 (2004).

¹³ N.N. Bogoliubov, Nuovo Cimento **7**, 794 (1958).

¹⁴ A. Mastellone, G. Falci, and R. Fazio, Phys. Rev. Lett. **80**, 4542 (1998).

¹⁵ J. von Delft and D.C. Ralph, Phys. Rep. **345**, 61 (2001).

¹⁶ P. Mohanty *et al.*, Physica C **408**, 666 (2004).

¹⁷ C.C. Tsuei and T. Doderer, The European Physical Journal B **10**, 257 (1999); C.J. Chen and C.C. Tsuei, Solid State Commun. **71**, 33 (1989); H.L. Edwards *et al.*, Phys. Rev. Lett. **73**, 1154 (1994); H.L. Edwards, *ibidem* **75**, 1387 (1995); S. Mori, C.H. Chen, and S.-W. Cheong, Phys. Rev. Lett. **81**, 3972 (1998).

¹⁸ R.W. Richardson and N. Sherman, Nucl. Phys. **52**, 221 (1964); *ibid.*, **52**, 253 (1964).

¹⁹ F. H. L. Essler, *et al.* *The One-Dimensional Hubbard Model*, (Cambridge University Press, 2005).

²⁰ E.H. Lieb and F.Y. Wu, Phys. Rev. Lett. **20** 1445 (1968).

²¹ For the same limit in the Bethe equations of the δ -interacting bose-gas see M.T. Batchelor, X.W. Guan, and J.B. McGuire, J. Phys. A **37** (2004) L497; M.T. Batchelor, *et al.*, J. Phys. Soc. Jpn. **74** Suppl. 53-56 (2005).

²² J. Dukelsky, S. Pittel, G. Sierra, Rev. Mod. Phys. **76**, 643 (2004).

²³ L. Amico, G. Falci, and R. Fazio, J. Phys. A **34**, 6425 (2001); A. Di Lorenzo *et al.*, Nucl. Phys. B, **644**, 409 (2002).

²⁴ M.C. Cambiaggio, A.M.F. Rivas, and M. Saraceno, Nucl. Phys. A **624**, 157 (1997).

²⁵ H.J. Schulz and B.S. Shastry, Phys. Rev. Lett. **80**, 1924 (1998).

²⁶ A. Osterloh, L. Amico and U. Eckern, Nucl. Phys. B **588**, 531 (2000).

²⁷ M. Gaudin “Travaux de M. Gaudin: Modèles Exactement résolus”, Les Editions de Physique, France, 1995.

²⁸ R.W. Richardson, J. Math. Phys. **18**, 1802 (1977).

²⁹ L. Amico *et al.*, Annals of Physics **299**, 228 (2002).

³⁰ L. Amico and A. Osterloh, Phys. Rev. Lett. **88**, 127003 (2002).

³¹ E. Sklyanin, Lett. Math. Phys. **47**, 275 (1999).